

Stochastic energetics of a Brownian motor and refrigerator driven by non-uniform temperature

Ronald Benjamin*

*Department of Chemical and Biological Engineering,
University of Colorado, Boulder, Colorado 80309, USA*

(Dated: March 23, 2019)

The energetics of a Brownian motor and refrigerator driven by position dependent temperature, known as the Büttiker-Landauer motor and refrigerator, is investigated by extensive numerical simulations of the inertial Langevin equation. Our results are qualitatively different compared to previous works based on the overdamped Langevin equation and other phenomenological approaches. We find that the irreversible heat transfer via kinetic energy greatly reduces the efficiency/coefficient of performance of the motor/refrigerator. The motor and refrigerator work with maximum efficiency and coefficient of performance at optimal values of mass and friction coefficient but can never reach the Carnot efficiency/coefficient of performance. We also study the behavior of the motor in the linear response regime under condition of maximum power and find that efficiency at maximum power can never reach the efficiency of an endoreversible engine working at maximum power: the Curzon-Ahlborn efficiency. Under an analogous condition equivalent to that of maximum power, the coefficient of performance of the refrigerator cannot reach the coefficient of performance reached by a Carnot engine. Predictions of linear irreversible thermodynamics are in good agreement with numerical data. Finally, we investigate the role of different potential and temperature profiles to reduce the irreversible kinetic energy contribution, and increase the motor efficiency and refrigerator coefficient of performance. Our simulations show that optimizing the potential and temperature profile in order to reduce the irreversible heat transfer, diminishes the particle current as well leading only to a marginal enhancement of the system performance.

PACS numbers: 05.10.Gg, 05.40.Jc, 05.70.Ln

I. INTRODUCTION

Technology has moved to an era where the creation and manipulation of devices at the nanoscale regime has become increasingly possible. At the nanoscale regime, the nanomachine is subject to thermal fluctuations which might seem to pose a hindrance for its functioning. However, it is known that thermal noise can also play a beneficial role in the working of certain small scale devices. One example of such nanoscale devices is that of Brownian motors [1], which do useful work by rectifying thermal fluctuations. Since at equilibrium, the principle of detailed balance rules out any net flux, unidirectional motion can be achieved only when the system is driven away from equilibrium.

The source of non-equilibrium could be an external system providing energy such as a time-dependent force or if the system is subject to a thermal gradient. Examples of the latter kind of Brownian motors are the autonomous thermal motors such as the Feynman-Smoluchowski (FS) motor [2], where the system is simultaneously under the influence of two thermal reservoirs at different temperatures and the Büttiker-Landauer (BL) motor [3, 4], where the Brownian particle is alternately attached along the spatial coordinate, to thermal baths at different temperatures. Thermodynamic quantities such as the work output and efficiency, which characterize how effectively

such microscopic engines perform their tasks, have been a widely studied topic in recent years [5].

The energetics and transport properties of the BL motor have been studied by many authors. Landauer [3], first proposed the idea of the BL motor when he showed the physical significance of nonuniform temperature in changing the relative stability of otherwise locally stable states, a phenomenon he termed as the “blow-torch” effect. Such a position dependent temperature can also induce a net transport of Brownian particles in a periodic potential [3, 4, 6]. Due of the asymmetry created by the nonuniform temperature, the Brownian particle can more easily climb the potential barrier when it is in a hot region than when it is in the cold region. As a result, in the steady state we find a net flux of Brownian particles along with a heat transfer in the same direction as the temperature gradient. In the presence of a small external load it can also do some work as a motor or heat engine.

While a thermal gradient can create a net movement of Brownian particles, Onsager symmetry tells us that there will be a reciprocal process of the BL motor, namely the BL refrigerator. In presence of uniform temperature and an external force, there will be a heat flow from one thermal bath to the other, leading to cooling in one bath. In presence of a temperature difference, and an external load of magnitude greater than the stall load, the Brownian particles can transfer heat from the cold to the hot bath, like a heat pump [7, 8, 9].

Stochastic energetics formulated by Sekimoto [10], for mesoscale systems dominated by thermal fluctu-

*Electronic address: Ronald.Benjamin@Colorado.EDU

ations, has been applied to investigate the efficiency of the BL motor/refrigerator. This led to a debate regarding the maximum attainable thermodynamic efficiency/coefficient of performance of the BL motor/refrigerator. It was shown, using overdamped models that the BL motor can reach Carnot efficiency and the BL refrigerator can attain the corresponding Carnot coefficient of performance [7, 8, 11]. However, Derényi-Astumian [12] and Hondou-Sekimoto [13] argued that Carnot efficiency is unattainable due to the irreversible heat flow via kinetic energy. They made phenomenological predictions regarding the failure of overdamped models in predicting this heat transfer. In a recent work [14], we confirmed Sekimoto's stochastic energetics for non-uniform temperature as well as the predictions of Derényi-Astumian [12] and Hondou-Sekimoto [13], using first principles molecular dynamics simulation and numerical solution of the Langevin equation, taking inertia into account. We also found that the irreversible heat transfer via the kinetic energy greatly reduces the efficiency of the motor.

The kinetic energy contribution will also affect the refrigerator performance in presence of non-uniform temperature as the irreversible heat transfer from the hot to the cold reservoir would reduce the amount of heat extracted from the cold bath thus diminishing the coefficient of performance.

Various authors have studied the thermodynamics of the BL motor and refrigerator using overdamped models [7, 8] and other phenomenological approaches [9]. In the present work, we will discuss the energetics of the system by extensive numerical simulation of the inertial Langevin equation also compare the results in a few cases with first principles molecular dynamics simulation. We will also investigate the effect of different potential shapes and temperature profiles on the kinetic energy contribution and whether the performance of the BL motor and refrigerator can be enhanced using this approach.

Since a real motor must deliver a finite amount of work in a finite time, it is interesting from a practical viewpoint to also analyze its efficiency under the condition of maximum power. In a recent work, Van den Broeck [15] has shown that in the linear response regime, the efficiency at maximum power of a Brownian motor can attain the efficiency of an endoreversible engine when it operates at maximum power, namely the Curzon-Ahlborn efficiency if the condition of "tight coupling" is satisfied [16]. The efficiency at maximum power of the BL motor has also been studied using overdamped models [7] and the authors showed that it is close to the Curzon-Ahlborn efficiency. Corresponding to the efficiency at maximum power, some authors have studied the equivalent quantity for the refrigerator using linear irreversible thermodynamics [17]. Since the overdamped model fails to predict the correct heat transfer, we will examine the linear response behavior of the system by taking the inertia of the Brownian particle into account.

The paper has been organized as follows: In the next

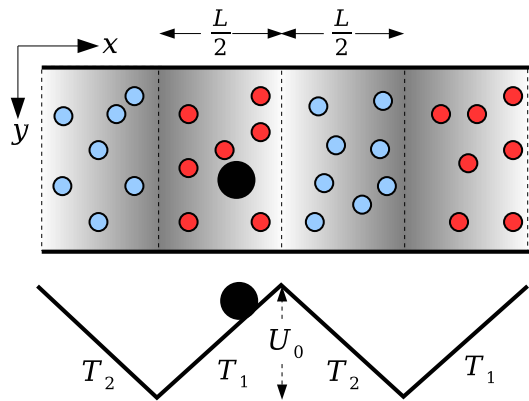


FIG. 1: (Color online) Two rectangular reservoirs filled with gas particles at temperatures T_1 and T_2 are alternately connected. Gas particles [red (dark gray) and blue (light gray) circles] are confined in the cell and only Brownian particles (large black circle) can move through the walls. Brownian particles are subjected to a piece-wise linear potential as shown in the bottom.

section we introduce the basic model, as studied in our previous work [14], and the methods used to investigate the energetics of the BL motor and refrigerator. In sections III and IV, we discuss the efficiency and performance of the BL motor and refrigerator respectively based on the basic model. Section V discusses the efficiency and coefficient of performance in the linear response regime. In section VI, we study the effect of different potential and temperature profiles on the motor efficiency and refrigerator coefficient of performance. Finally, we end with a conclusion.

II. BASIC MODEL AND METHODS

We consider a chain of two-dimensional cells attached to each other along the x direction (see Fig. 1). Each cell is $L/2$ long and filled with N gas particles of mass m . The cells are thermally isolated from each other and at thermal equilibrium with a temperature independent from the neighboring cells. Brownian particles of mass M are placed in the cells and, unlike the gas particles, can move through the cell walls. They are also subjected to a periodic piece-wise linear potential $U(x)$ with a period L in the x direction and constant in the y direction. For simplicity, we use a piecewise-linear potential:

$$U(x) = \begin{cases} -\frac{2U_0}{L}x & \text{for } -\frac{L}{2} < x \leq 0, \\ \frac{2U_0}{L}x & \text{for } 0 < x \leq \frac{L}{2}, \end{cases} \quad (1)$$

where U_0 is the potential height. In addition to the periodic potential, a constant external force F is exerted on the Brownian particles. Instead of infinitely long chains we consider only two cells with a periodic boundary condition: cell 1 with temperature T_1 for $-L/2 < x \leq 0$ and cell 2 with T_2 for $0 < x \leq L/2$.

Apart from long-time fluid dynamical effects in two dimensions, the motion of the Brownian particle in the x direction can be investigated by the one-dimensional Langevin equation:

$$\begin{aligned} \dot{x} &= v, \\ M\dot{v} &= -\gamma(x)v - U'(x) + F + \sqrt{2\gamma(x)T(x)}\xi(t), \end{aligned} \quad (2)$$

where x and v are the position and velocity of the Brownian particle and $\xi(t)$ is a standard Gaussian white noise:

$$\langle \xi(t) \rangle = 0, \quad \langle \xi(t)\xi(s) \rangle = \delta(t-s). \quad (3)$$

The piecewise constant temperature is given by:

$$T(x) = \begin{cases} T_1 & \text{for } -\frac{L}{2} < x \leq 0, \\ T_2 & \text{for } 0 < x \leq \frac{L}{2}. \end{cases} \quad (4)$$

Temperature is measured in energy unit ($k_B = 1$). Here, and later on, an overdot refers to derivative taken with respect to time and a prime means derivative taken with respect to space. Assuming that Einstein's relation, namely, $D(x) = T(x)/\gamma(x)$ holds locally, the friction coefficient also depends on the position in the same way as the temperature through the relation

$$\gamma(x) = \rho\sigma_B\sqrt{2\pi T(x)m}, \quad (5)$$

where, ρ is the number density of gas particles in a cell. The above analytical expression for $\gamma(x)$ holds for an ideal gas [18].

When the relaxation time $\tau = M/\gamma$ is much smaller than a mechanical time scale $t_0 = \sqrt{ML^2/U_0}$, the inertia of the Brownian particle may be neglected, allowing the use of the overdamped Langevin equation. However, we confirmed in our previous work [14] that the overdamped model fails in predicting the heat transfer when temperature is inhomogeneous. Therefore, we use the inertial Langevin equation (2) and compare the results with molecular dynamics simulation.

In our MD simulation, both gas and Brownian particles are hard disks of diameter σ and σ_B , respectively. A cell of size 250×400 ($L = 500$) contains 1000 gas particles so that $\rho = 0.01$, low enough to use the Langevin equation. For convenience, we assume $m = 1$, $\sigma = 1$ and $U_0 = 1$. See Ref. [14] for the detailed algorithm of the simulation.

In order to investigate the thermodynamic properties, we use stochastic energetics formulated by Sekimoto [10, 19, 20]. The heat flux from the gas particles in the i -th cell to the Brownian particles is defined as,

$$\dot{Q}_i = \left\langle \left(-\gamma_i \dot{x} + \sqrt{2\gamma_i T_i} \xi(t) \right) \dot{x} \right\rangle_i, \quad (6)$$

where, $\langle \cdots \rangle_i$ indicates ensemble average taken while the Brownian particles are located in the i -th cell. Using the Langevin equation (2), we obtain the total heat flux as a sum of three terms:

$$\begin{aligned} \dot{Q}_i &= \frac{M}{2} \frac{d}{dt} \langle \dot{x}^2 \rangle_i + \langle U'(x) \dot{x} \rangle_i - F \langle \dot{x} \rangle_i \\ &= \dot{Q}_i^{\text{KE}} + \dot{Q}_i^{\text{PE}} + \dot{Q}_i^{\text{J}} \end{aligned} \quad (7)$$

where the first two terms on the rhs are the kinetic energy and potential energy contribution to the heat flux, respectively, and the last term is the Joule heat. Work done on a Brownian particle by the external force F in each cell is given by,

$$\dot{W}_i = F \langle \dot{x} \rangle_i. \quad (8)$$

and the total work done on the Brownian particle is given by,

$$\dot{W} = F(\langle \dot{x} \rangle_1 + \langle \dot{x} \rangle_2) = F \langle \dot{x} \rangle \quad (9)$$

where, $\langle \dot{x} \rangle_1 = \langle \dot{x} \rangle_2 = \langle \dot{x} \rangle / 2$, since width of both cells are the same.

In the steady state, the net energy flux to the Brownian particles will vanish, and thus the energy gained by the Brownian particles in cell 1 will be cancelled by the energy loss in cell 2. Therefore, heat flux from cell 1 to cell 2 via the Brownian particles is defined as

$$\begin{aligned} \dot{Q}_{1 \rightarrow 2} &= \dot{Q}_1 + \dot{W}_1 = \dot{Q}_1^{\text{KE}} + \dot{Q}_1^{\text{PE}} \\ &= -\dot{Q}_2 - \dot{W}_2 = -\dot{Q}_2^{\text{KE}} - \dot{Q}_2^{\text{PE}}. \end{aligned} \quad (10)$$

III. EFFICIENCY OF THE MOTOR

When two cells have different temperatures ($T_1 > T_2$), the Brownian particles in the higher temperature cell can reach the higher-potential energy region more often than those in the low-temperature cell. Hence, the Brownian particles tend to move from the hot to the cold cell over the potential barrier, resulting in a net current in the positive direction even in the absence of an external force ($F = 0$). In the presence of an external load ($F < 0$), the Brownian particles can do work against it behaving as a motor. In this section, we discuss the thermodynamic efficiency of the BL motor, defined as

$$\eta = \frac{-\dot{W}}{\dot{Q}_1}. \quad (11)$$

In Fig. 2, we plot the motor velocity, rate of work output or the power $-\dot{W}$, various components of the heat flow out of cell 1 at temperature T_1 , and efficiency as a function of the external load. As the external load impedes the motion of the motor, the velocity decreases and vanishes at the stall load F_{stall} . When $F = 0$, the average velocity of the Brownian particles is not zero, but the work is zero. At the stall load, since the motor velocity goes to zero, the work output again vanishes. At a certain value of F , between 0 and F_{stall} , the work output reaches a maximum i.e., the motor delivers maximum power.

Now we come to the heat transfer. When the Brownian particle crosses one period to the right it extracts potential energy U_0 from the higher-temperature cell at the rate $(2U_0/L)\langle \dot{x} \rangle_1$ and dissipates the same amount of potential energy to the cold cell. This heat flow via potential decreases with the load as the velocity decreases

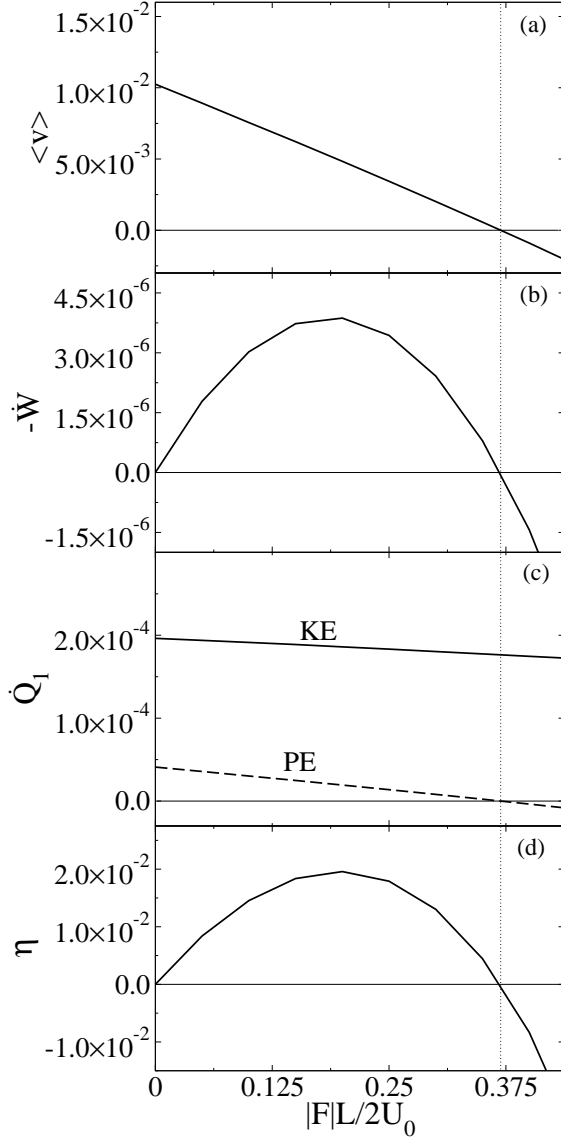


FIG. 2: (a) Average velocity $\langle v \rangle$, (b) power $-\dot{W}$, (c) \dot{Q}_1^{KE} and \dot{Q}_1^{PE} , and (d) efficiency of the motor as a function of $|F|L/2U_0$. In (a), (b), (c) and, (d) the thin horizontal solid line represents $y = 0$. The parameter values are $T_1 = 0.7$, $T_2 = 0.3$, $\sigma_B = 5$ and $M/m = 5$. The Carnot efficiency $\eta_c = 0.57$.

and ultimately vanishes at F_{stall} . At the quasistatic limit of zero motor velocity, this heat transfer via potential energy is reversible.

On the other hand, Fig. 2 shows that the heat flow via kinetic energy varies slowly with the load and is positive even in the quasistatic limit, showing that a net heat flows from the hot to the cold reservoir even when the motor does not deliver any work. As explained in our previous work [14], when the Brownian particle crosses a temperature boundary from the hot to the cold side it dissipates heat due its kinetic energy, to the cold bath. This

kinetic energy contribution will be proportional to the temperature difference between the hot and cold baths. Even when the velocity of the Brownian particles is zero, they are still crossing the temperature boundary back and forth. Therefore, this heat continues to flow at the stall load. Since the heat flows always from the hot cell to the cold cell, independent of the direction of the Brownian particle's movement, it is irreversible heat.

The presence of this entropy producing irreversible heat carried by the kinetic energy of the Brownian particle, makes it impossible for the BL motor to reach Carnot efficiency $\eta_c = 1 - T_1/T_2$. In fact, Fig. 3 shows that the efficiency is a magnitude order lower than η_c and diminishes to zero at the quasistatic limit (at the stall load).

Figure 3 shows the power, heat flow via kinetic energy, and motor efficiency as a function of the temperature difference between the two cells. Overdamped models [7], which ignore the kinetic energy contribution, predict that the efficiency increases with ΔT and then saturates. However, when we take inertia into account its a different story. We find that at smaller ΔT the work output is low leading to a low efficiency while at large ΔT , the heat flow via kinetic energy is large, again reducing the efficiency. Figure 3 also shows that the kinetic energy is proportional to the temperature difference between the cells, since greater is the temperature difference between the cells, greater is the difference between the average kinetic energy of the Brownian particle in the hot and cold cells. There is an optimum ΔT at which the efficiency is maximum but it is far lower than the Carnot efficiency.

We had shown in our previous paper [14] that \dot{Q}^{KE} diverges as $M^{-1/2}$ in the overdamped limit ($M \rightarrow 0$). This can be understood as follows: the Brownian particle thermalizes over a length scale $\ell_{th} = v_{th}\tau = \sqrt{TM}/\gamma$, where $v_{th} = \sqrt{T/M}$ is the thermal velocity. Within this thermal length scale, the average kinetic energy of the Brownian particle deviates from the bath temperature. If, we are in the overdamped regime and the width of the cells is much larger than the thermal length scales then, away from the border region between the hot and cold baths the kinetic energy of the Brownian particle is adapted to the local bath temperature [13]. However, in the narrow transition region between the two baths the average kinetic energy of the particle will gradually decrease from $T_1/2$ inside the hot bath to $T_2/2$ inside the cold bath (see the kinetic energy profile in Fig.3 of Ref. [14]).

The kinetic energy contribution, as Fig. 3 shows, is proportional to the temperature difference between the cells. As the temperature is non-uniform, the kinetic energy contribution will consequently be proportional to the effective temperature gradient: $|T_1 - T_2|/\ell_{th} \propto M^{-1/2}$. As we approach the overdamped limit, the length of the transition region decreases and the average kinetic energy profile of the Brownian particle in this transition region becomes more and more steep. In the overdamped limit ($M \rightarrow 0$), the change in the average kinetic energy will be sudden as the transition region vanishes and hence the

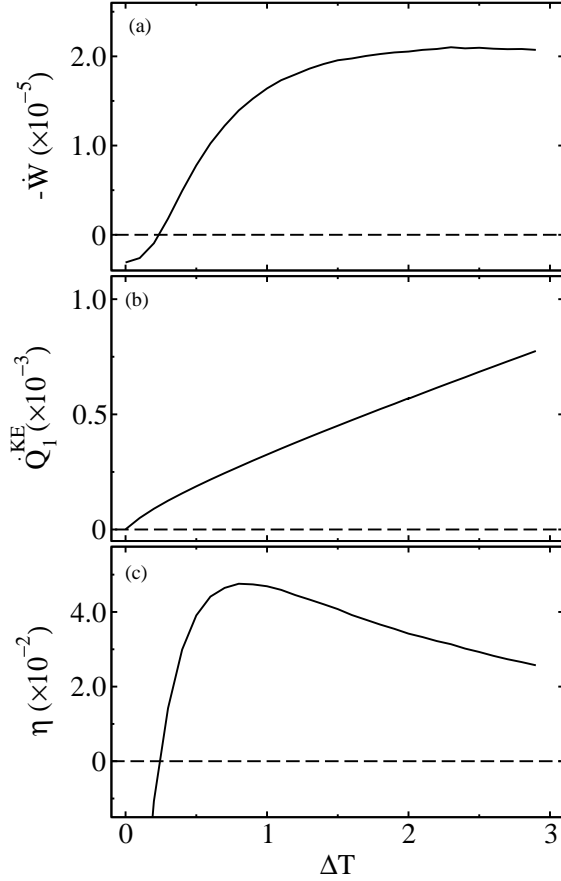


FIG. 3: (a) Power, (b) heat flux due to kinetic energy, and (c) efficiency as a function of $\Delta T = T_1 - T_2$, where T_2 is kept at 0.1. The parameter values are $M/m = 5.0$, $|F|L/2U_0 = 0.5$ and $\sigma_B = 5.0$. In (a), (b) and, (c) the thin horizontal dashed line represents $y = 0$. The Carnot efficiency varies from 0.67 at $\Delta T = 0.2$ to 0.96 at $\Delta T = 2.8$.

effective thermal gradient tends to infinity and the irreversible heat transfer diverges as $M^{-1/2}$. Since this irreversible heat dominates the heat flow via potential, the efficiency diminishes to zero as \sqrt{M} , in the overdamped limit. This was also predicted by Derényi-Astumian[12].

On the other hand, in the underdamped limit ($M \rightarrow \infty$), the Brownian particle doesn't thermalize to the local environment before entering the next heat bath [21] and the motor fails, diminishing the power and efficiency to zero. The efficiency will be maximum at an optimal value of M . Figure 4, clearly confirms these predictions. We also find good agreement between the inertial Langevin equation and molecular dynamics simulation, suggesting the validity of Sekimoto's stochastic energetics for non-uniform temperature.

We now study the effect of friction coefficient on the energetics. In Fig. 5 we plot the power, heat flow via kinetic energy and efficiency as a function of the friction coefficient. In the underdamped regime ($\gamma(x) \ll 1$), the kinetic energy of the Brownian particle does not equilibrate

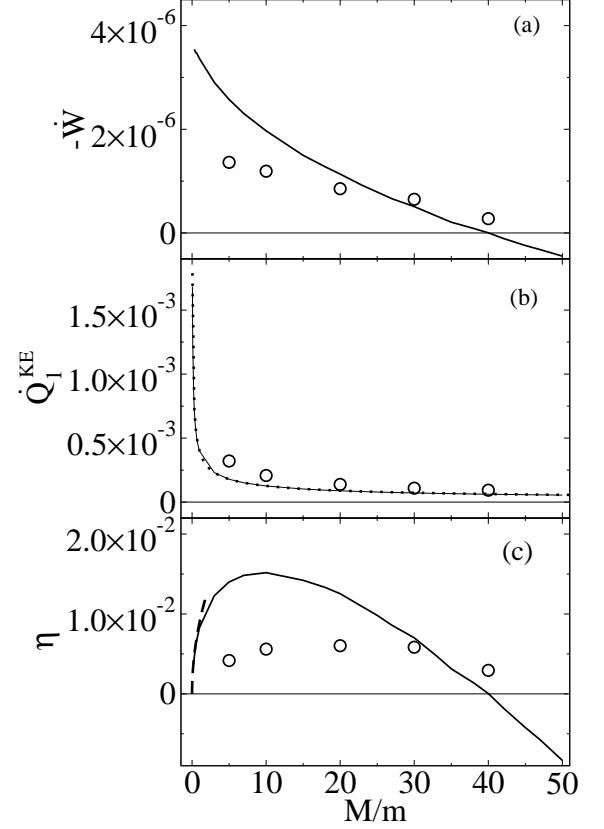


FIG. 4: (a) Power, (b) heat flux due to kinetic energy, and (c) efficiency as a function of the mass ratio M/m . Symbols and lines correspond to MD simulation and the inertial Langevin equation respectively. The dotted line in (b) corresponds to a phenomenological fit ($\propto M^{-1/2}$) to the kinetic energy contribution. The dashed line in (c) represents a fit ($\propto \sqrt{M}$) to the efficiency in the overdamped limit ($M \rightarrow 0$). In (a), (b) and, (c) the thin horizontal solid line represents $y = 0$. The parameter values are $T_1 = 0.7$, $T_2 = 0.3$, $|F|L/2U_0 = 0.3$ and $\sigma_B = 5.0$. The Carnot efficiency $\eta_c = 0.57$.

to the bath temperature and hence the asymmetry due to the inhomogeneous temperature becomes negligible. As a result, a positive current cannot be sustained against the load, and the motor fails to deliver work. Similarly, in the overdamped limit ($\gamma(x) \rightarrow \infty$) the large friction coefficient makes the Brownian particle immobile and the work output again goes to zero.

However, the irreversible heat flow via kinetic energy shows a different behavior as the friction coefficient increases. As the medium becomes more damped, the Brownian particle tends to adapt to the local bath temperature so that its average kinetic energy in each cell approaches $T_i/2$ ($i = 1, 2$). Since, the kinetic energy contribution $Q_{1 \rightarrow 2}^{\text{KE}}$, is proportional to the difference between the average kinetic energy of the Brownian particle in the two cells, it increases with the damping and saturates in the overdamped limit, confirming Hondou and Seki-

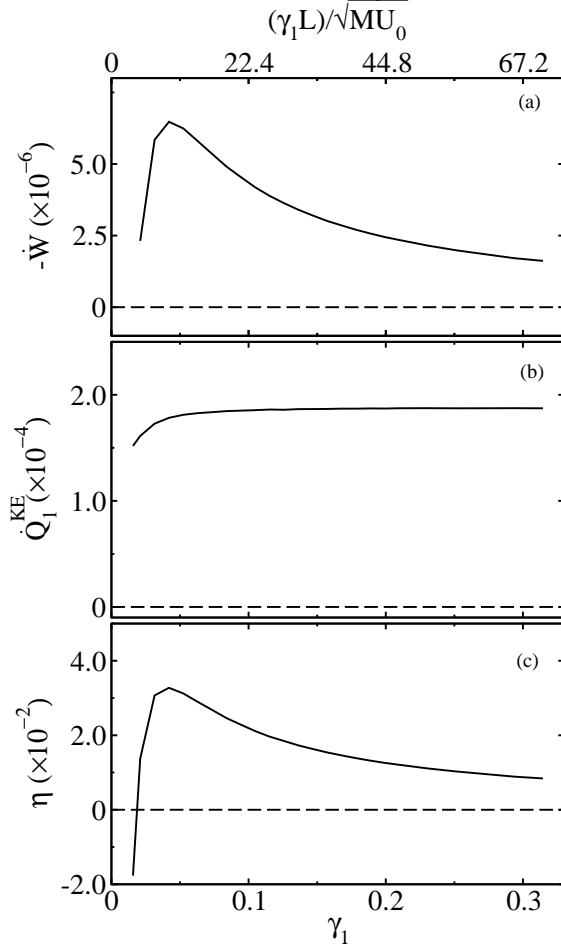


FIG. 5: (a) Power, (b) heat flux due to kinetic energy and, (c) efficiency as a function of γ_1 . The parameter values are $T_1 = 0.7$, $T_2 = 0.3$, $|F|L/2U_0 = 0.2$ and $M/m = 5.0$. In (a), (b) and, (c) the thin horizontal dashed line represents $y = 0$. The friction coefficient is varied by increasing the diameter of the Brownian particle. The Carnot efficiency $\eta_c = 0.57$. The top x -axis in (a) shows the dimensionless friction coefficient $\gamma_1 L / \sqrt{MU_0}$, as an indicator of the friction regime. Typically, $\gamma_1 L / \sqrt{MU_0} > 10$ corresponds to the overdamped regime and $\gamma_1 L / \sqrt{MU_0} \lesssim 1$ corresponds to the underdamped regime.

moto's conjecture that the kinetic energy contribution is independent of the friction coefficient in the overdamped regime. Finally, Figure 5 shows that there is an optimum friction coefficient at which the efficiency is maximum.

IV. PERFORMANCE OF REFRIGERATOR

We now discuss the energetics of the BL refrigerator. When the external load exceeds the stall load, the motor will move backward in the same direction as F . In this situation, some authors [7, 8, 9] have claimed that the Brownian particle will transfer heat against the temperature gradient, from the cold to the hot bath, func-

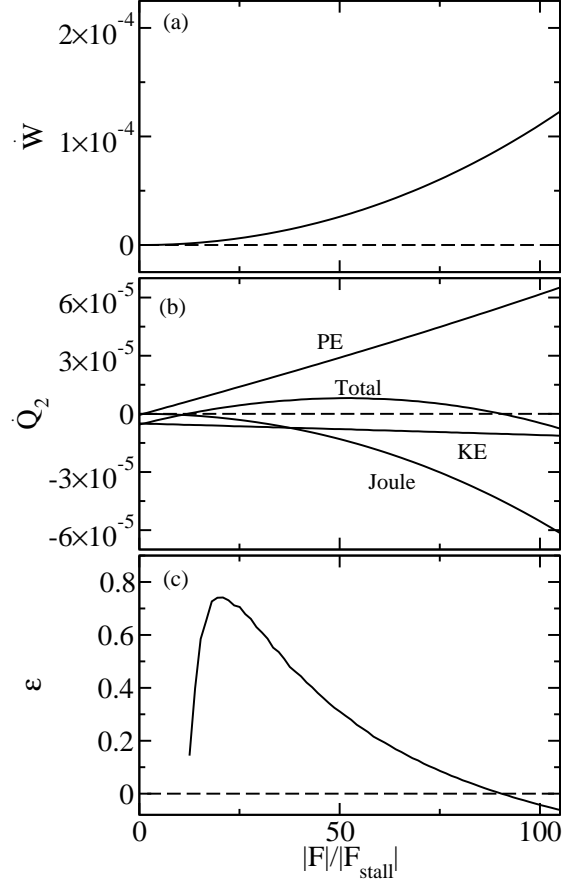


FIG. 6: (a) Work input \dot{W} , (b) various components of \dot{Q}_2 (from top to bottom the heat flows are \dot{Q}_2^{PE} , \dot{Q}_2 , \dot{Q}_2^J and \dot{Q}_2^{KE}), and (c) the coefficient of performance ε as a function of F/F_{stall} , F_{stall} being the stall load. In (a), (b) and, (c) the thin horizontal dashed line represents $y = 0$. The parameter values are $\Delta T = T_1 - T_2 = 0.01$, $T_2 = 0.5$, $M/m = 5.0$ and $\sigma_B = 5.0$. The Carnot coefficient of performance $\varepsilon_c = 50$.

tioning as a refrigerator, and at the stalled state the coefficient of performance ε , defined as,

$$\varepsilon = \frac{\dot{Q}_2}{\dot{W}}, \quad (12)$$

will attain the Carnot coefficient of performance $\varepsilon_c = T_2/(T_1 - T_2)$.

In Fig. 6, we plot the heat flow out of the hot and cold cells as a function of the external load. In contradiction to the claim made in Refs. [7, 8, 9], we find that the stalled state, at which the current changes its direction is not the transition point from the motor to the refrigerator. At the stalled state, the heat flow via potential, which follows the direction of the particle flux $\langle v \rangle$, goes to zero. However, there is still a net heat transfer from the hot to the cold cell due to the kinetic energy contribution. In fact, the heat flow via kinetic energy never vanishes and always flows from the hot to the cold reser-

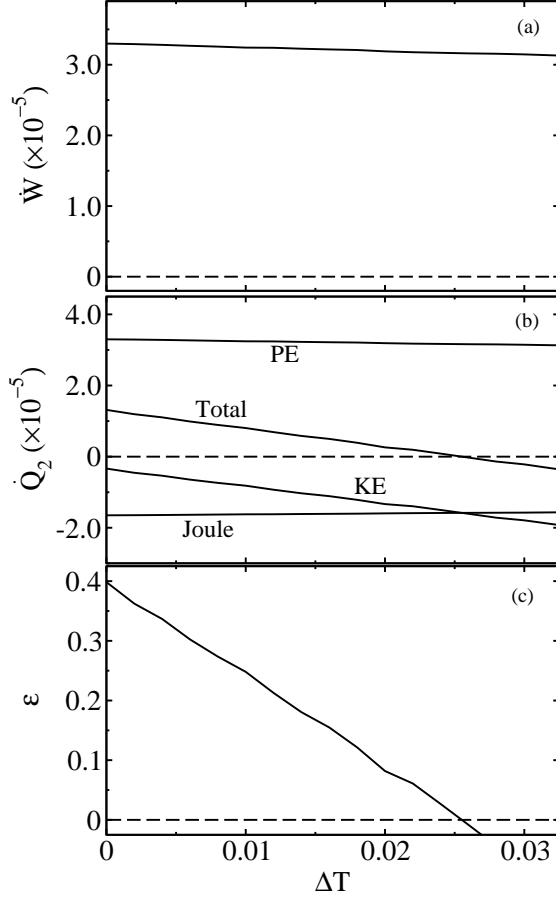


FIG. 7: (a) \dot{W} , (b) various components of \dot{Q}_2 (from top to bottom the heat flows are \dot{Q}_2^{PE} , \dot{Q}_2 , \dot{Q}_2^{KE} and \dot{Q}_2^{J}) and, (c) the coefficient of performance ε as a function of ΔT for $M/m = 5.0$, $\sigma_B = 5.0$, $|F|L/2U_0 = 0.5$. In (a), (b) and, (c) the thin horizontal dashed line represents $y = 0$. Temperature of the cold bath is kept constant at $T_2 = 0.5$ and T_1 is varied. ε_c varies from ∞ at $\Delta T = 0$ to 20 at $\Delta T = 0.025$.

voir regardless of the direction of particle current and magnitude of the external load.

Figure 6 shows that starting from the stall load there is a region where the model works neither as a motor nor as a refrigerator i.e., heat flows from the hot to the cold cell and work is done on the Brownian particle. Refrigeration starts only when the heat flow via potential exceeds the sum of joule heat dissipated to the cold bath and the heat transfer via kinetic energy. As the load is further enhanced, the joule heat (varying as $|F|^2$), which originates from the power supply \dot{W} , eventually dominates the heat flow via potential (varying as $|F|$) and the cooling stops. There is an optimal load at which the heat flow out of the cold cell and the coefficient of performance attain a maximum but ε is far below ε_c , due to the heat flow via kinetic energy.

In Fig. 7, we show the power supply, various components of the heat transfer from the cold bath at temper-

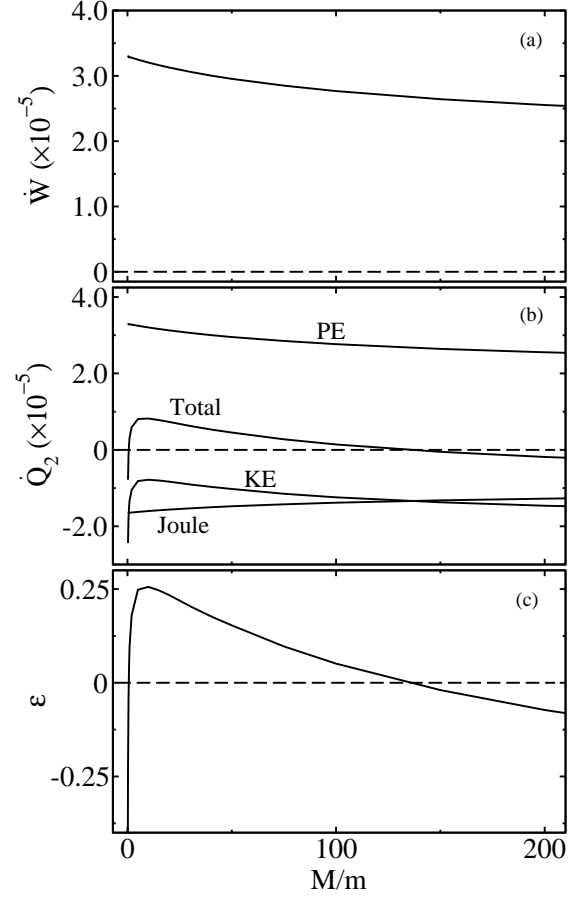


FIG. 8: (a) \dot{W} , (b) various components of \dot{Q}_2 (from top to bottom the heat flows are \dot{Q}_2^{PE} , \dot{Q}_2 , \dot{Q}_2^{KE} and \dot{Q}_2^{J}) and, (c) the coefficient of performance ε as a function of M/m for $\Delta T = 0.01$, $\sigma_B = 5.0$, $|F|L/2U_0 = 0.5$, $T_1 = 0.51$, $T_2 = 0.5$. In (a), (b) and, (c) the thin horizontal dashed line represents $y = 0$. The Carnot coefficient of performance is $\varepsilon_c = 50$.

ature T_2 and the coefficient of performance as a function of the temperature difference between the cells. We keep T_2 constant and vary T_1 . As the temperature difference between the baths increases, the net negative current in the direction of F will decrease as the increasing temperature of the hot bath will try to drive the Brownian particle in the forward direction. This decreases the heat flow via potential, which is proportional to the current, and hence the refrigerator's ability to transfer heat against the thermal gradient. The power supply and joule heat also decrease with ΔT . However, as $\Delta T \ll 1$, this decrease is marginal. On the other hand, the irreversible heat dumped to the cold cell via kinetic energy, increases significantly with ΔT and greatly reduces the cooling. In fact, beyond a small temperature difference $\Delta T \ll 1$, refrigeration fails, as Fig. 7 shows. The coefficient of performance is monotonically reduced with increasing temperature difference between the cells.

Figure 8 shows the power input, various components of

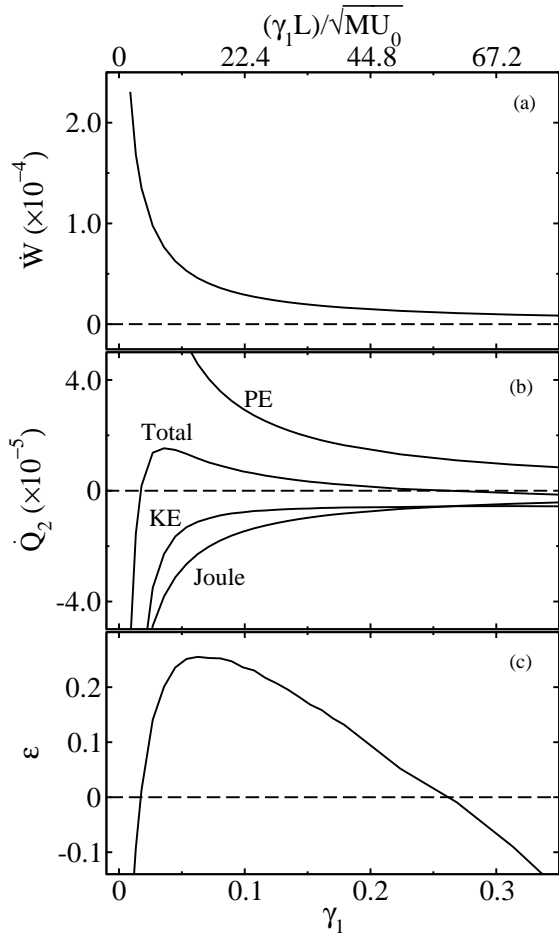


FIG. 9: (a) \dot{W} , (b) various components of \dot{Q}_2 (from top to bottom the heat flows are \dot{Q}_2^{PE} , \dot{Q}_2 , \dot{Q}_2^{KE} and \dot{Q}_2^{J}) and, (c) the coefficient of performance ε as a function of γ_1 for $\Delta T = 0.01$, $M/m = 5.0$, $|F|L/2U_0 = 0.5$, $T_1 = 0.51$, $T_2 = 0.5$. Carnot coefficient of performance $\varepsilon_c = 50$. In (a), (b) and, (c) the thin horizontal dashed line represents $y = 0$. The friction coefficient γ_1 is varied by increasing the diameter of the Brownian particle. The top x -axis in (a) shows the dimensionless friction coefficient $\gamma_1 L/\sqrt{MU_0}$, as an indicator of overdamping.

the heat flow and the coefficient of performance as a function of the mass of the Brownian particle. The larger the mass of the Brownian particle the larger is the intrawell relaxation time thus leading to a low particle current in the negative direction. Hence the heat flow via potential as well as the power input and joule heat decrease with the inertia of the Brownian particle. As expected, Fig. 8 shows that the irreversible heat via kinetic energy diverges in the overdamped limit. There is another component of the kinetic energy contribution, which goes to zero in the overdamped limit but becomes significant for large inertia. In the overdamped regime, the change in potential energy is immediately dissipated to the bath as the Brownian particle goes down the slope. However, at finite mass, the potential energy change is transported to

the next cell as an “unthermalized” kinetic energy contribution, where it is dissipated as heat. This “unthermalized” kinetic energy contribution increases with the mass of the Brownian particle [14]. Hence, the total heat flow and the coefficient of performance go to zero in both the underdamped and overdamped limits. There is an optimal mass of the Brownian particle at which \dot{Q}_2 and ε are maximized. But, ε is far below the Carnot limit.

In Fig 9 we plot \dot{W} , various components of \dot{Q}_2 and ε as a function of the friction coefficient. Since our numerical algorithm for solving the Langevin equation fails when $\gamma(x)L/\sqrt{MU_0} \rightarrow 0$, we could not reach the extreme underdamped limit $\gamma(x) \rightarrow 0$. In the underdamped regime, the “unthermalized” component of the kinetic energy is large, decreasing the total heat flow \dot{Q}_2 . In the overdamped limit, the kinetic energy contribution due to the temperature difference between the cells, saturates at a certain value. However, the large friction coefficient makes the Brownian particle almost immobile thus reducing the particle current and consequently the heat flow via potential. The work input and joule heat decrease as well. Hence, the coefficient of performance again diminishes to zero in both the overdamped and underdamped limits. There is an optimum friction coefficient at which \dot{Q}_2 and ε are maximum. However, ε is far below ε_c .

In our previous work [14], we had shown that when two cells have the same temperature and the Brownian particles are driven by an external force $F > 0$, we observe a net cooling in cell 1 at the expense of heating of cell 2. In Fig. 10, we show components of the heat flow from cell 1 to the Brownian particle and the coefficient of performance $\varepsilon = \dot{Q}_1/\dot{W}$ as a function of F when $T_1 = T_2$. We find that there is an optimal F at which \dot{Q}_1 is maximized. When temperature is uniform we do not expect any kinetic energy contribution. Hence it follows that ε will reach ε_c , which goes to ∞ when $T_1 = T_2$. Figure 10b shows that ε tends to infinity as $F \rightarrow 0$ which means that when temperature is uniform, a vanishingly small external force (or a power supply \dot{W} which goes to zero) is sufficient to generate a heat flow from cell 1 to cell 2. We also find good agreement between the inertial Langevin equation and the molecular dynamics simulation.

V. LINEAR IRREVERSIBLE THERMODYNAMICS

In this section we discuss the efficiency and coefficient of performance of the BL system in the linear response regime. The BL motor and refrigerator are a result of cross effect between the external force F and the temperature difference $\Delta T = T_1 - T_2$. If they are small, there exists a linear relationship between the thermodynamic fluxes ($\langle v \rangle$ and $\dot{Q}_{1 \rightarrow 2}$) and thermodynamic forces

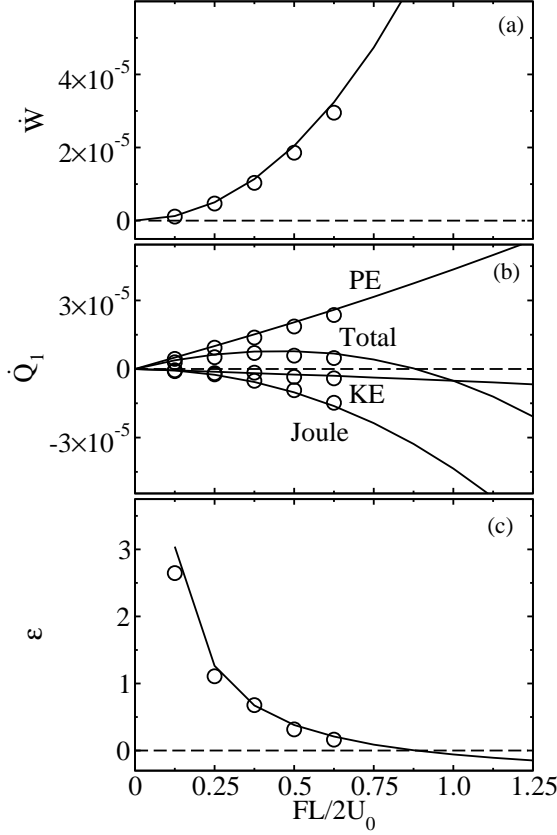


FIG. 10: (a) Work input, (b) various components of \dot{Q}_1 of the refrigerator as a function of $FL/2U_0$, (from top to bottom, the heat flows are \dot{Q}_1^{PE} , \dot{Q}_1 , \dot{Q}_1^{KE} and \dot{Q}_1^{J}), and (c) ϵ as a function of $FL/2U_0$, obtained from the inertial Langevin equation (lines) and molecular dynamics simulation (symbols). In (a), (b) and, (c) the thin horizontal dashed line represents $y = 0$. The parameter values are $T = 0.5$, $M/m = 20.0$ and $\sigma_B = 8.0$.

(F/T and $\Delta T/T^2$):

$$\begin{aligned} \langle v \rangle &= L_{11} \frac{F}{T} + L_{12} \frac{\Delta T}{T^2}, \\ \dot{Q}_{1 \rightarrow 2} &= L_{21} \frac{F}{T} + L_{22} \frac{\Delta T}{T^2}, \end{aligned} \quad (13)$$

where L_{ij} 's ($i, j = 1, 2$) are the Onsager transport coefficients, $T_1 = T + \Delta T/2$ and $T_2 = T - \Delta T/2$. While investigating the Büttiker-Landauer motor and refrigerator, we had shown in our previous work [14], the validity of linear irreversible theory and numerically confirmed Onsager symmetry relationship, namely $L_{12} = L_{21}$, for spatially inhomogeneous temperature.

The efficiency of the motor is given by,

$$\eta = \frac{-\dot{W}}{\dot{Q}_{1 \rightarrow 2}} = \frac{-F \left(L_{11} \frac{F}{T} + L_{12} \frac{\Delta T}{T^2} \right)}{L_{21} \frac{F}{T} + L_{22} \frac{\Delta T}{T^2}}. \quad (14)$$

Recently, Van den Broeck [22] investigated the efficiency of Brownian motors in the linear response regime and

concluded that, in principle, Carnot efficiency can be attained. He argued that for small F , the temperature difference ΔT drives the motor in the forward direction and simultaneously there is a heat transfer from the hot to the cold reservoir. As F increases, we ultimately reach the quasistatic condition of zero motor velocity at the stall load F_{stall} . From Eq. (13), we find that the stall load is given by,

$$F_{\text{stall}} = -\frac{L_{12}}{L_{11}} \left(\frac{\Delta T}{T} \right). \quad (15)$$

Beyond the stall load, the motor reverses its direction, transferring heat against the temperature gradient as a heat pump. In an ideal system, the velocity and heat reverse directions at the same value of F_{stall} so that $\langle v \rangle$ and $\dot{Q}_{1 \rightarrow 2}$ vanish for nonzero F and ΔT . Substituting the value of F_{stall} for F in Eq. (14), we find that this happens only when the condition of zero entropy production: $L_{11}L_{22} = L_{12}L_{21}$ holds, and Onsager symmetry relationship is valid. This condition is referred to as “tight coupling” condition and when it is satisfied, we find that efficiency at the quasistatic limit is equal to the Carnot efficiency: $\Delta T/T$.

Carnot efficiency, however, can only be reached in the quasistatic condition where the motor velocity is zero, and hence it does not deliver any work. In practice a motor, must perform finite work in a finite time. A more practical measure of the motor efficiency is the efficiency when it delivers maximum work. Curzon and Ahlborn [16] claimed that the efficiency at maximum power η^* is bounded by the Curzon-Ahlborn efficiency, $\eta_{\text{max}}^* = 1 - \sqrt{T_2/T_1}$, where $T_1 > T_2$. The claim was found to be valid for thermal motors [15]. Asfaw and Bekele [7] studied the efficiency at maximum power (η^*) of the BL motor and found that η^* approaches η_{max}^* as the temperature difference between the reservoirs $T_1 - T_2 = \Delta T \rightarrow 0$. However, their conclusions are not reliable since they used the overdamped model and also a different definition of work from the one used in the Carnot efficiency. In order to evaluate efficiency at maximum power, we must use the proper thermodynamic definition of work (Eq. (9)) and take into account the inertia of the Brownian particle into account.

Maximum power will be attained at a value of the load F^* given by,

$$F^* = -\frac{L_{12}}{L_{11}} \left(\frac{\Delta T}{2T} \right). \quad (16)$$

Substituting the value of F^* in Eq. (14), we find that the efficiency at maximum power is given by,

$$\eta_q^* = \frac{\Delta T}{2T} \frac{q^2}{2 - q^2}, \quad (17)$$

where,

$$q = \frac{L_{12}}{\sqrt{L_{11}L_{22}}}. \quad (18)$$

If the necessary condition of zero entropy production is satisfied, then $q = 1$ and to the lowest order of ΔT , the efficiency at maximum power approaches the efficiency of an endoreversible heat engine at maximum power viz., the Curzon-Ahlborn efficiency: $\eta_{max}^* = 1 - \sqrt{T_2/T_1} \sim \Delta T/2T$ [16]. However, in our previous work [14] we had shown that the product of the diagonal coefficients $L_{11}L_{22}$ diverges as $(M/m)^{-1/2}$, reflecting the divergence of the kinetic energy contribution. The off-diagonal coefficients however, did not show this singular behavior. Consequently, we find $L_{11}L_{22} \gg L_{12}L_{21}$ for all values of M/m indicating large entropy production and very low efficiency. Hence the BL motor can never attain the Carnot efficiency or the Curzon-Ahlborn efficiency.

The coefficient of performance of the refrigerator is given by,

$$\varepsilon = \frac{-\dot{Q}_{1 \rightarrow 2}}{\dot{W}} = \frac{-L_{21}\frac{F}{T} - L_{22}\frac{\Delta T}{T^2}}{F\left(L_{11}\frac{F}{T} + L_{12}\frac{\Delta T}{T^2}\right)} \quad (19)$$

By similar arguments as in the case of the motor, it is easy to show that the coefficient of performance reaches the Carnot coefficient of performance $T/\Delta T$ in the quasistatic limit, only if the necessary condition $L_{11}L_{22} = L_{12}L_{21}$ holds.

In the quasistatic limit, the refrigerator does not transfer any heat and hence is practically useless. Since Carnot coefficient of performance is only possible in the quasistatic limit, it is not an effective measure of the refrigerator performance from a practical point of view. A refrigerator must transfer a finite amount of heat in a finite time. Similar to the efficiency at maximum power for the motor we must find the coefficient of performance of the refrigerator, under conditions of finite heat transfer from the cold to the hot bath. Following Van den Broeck's work [15], regarding the efficiency at maximum power for the motor, some authors have investigated the coefficient of performance of the refrigerator at maximum $\dot{Q}_{1 \rightarrow 2}(\Delta T/T)$ [17]. This quantity is maximum at a temperature difference ΔT^* , given by

$$\Delta T^* = -\frac{L_{21}}{L_{22}} \frac{FT}{2}. \quad (20)$$

Substituting the value of ΔT^* in place of ΔT in Eq.(19), we find that up to the lowest order of ΔT , the coefficient of performance at maximum $\dot{Q}_{1 \rightarrow 2}(\Delta T/T)$, is given by

$$\varepsilon_q^* = \frac{q^2}{2 - q^2} \frac{T}{2\Delta T} \quad (21)$$

Analogous to the efficiency at maximum power, ε^* is equal to a factor that depends on q only, times half the Carnot coefficient of performance. If the necessary condition for attaining the Carnot coefficient of performance, namely $L_{11}L_{22} = L_{12}L_{21}$ holds, then $q = 1$ and ε^* attains a maximum ε_{max}^* given by,

$$\varepsilon_{max}^* = \frac{T}{2\Delta T} \quad (22)$$

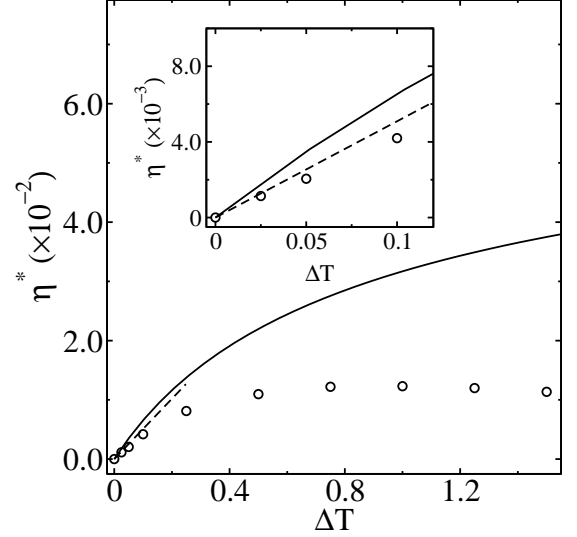


FIG. 11: η^* (symbols), η_q^* (dashed line) and the Curzon-Ahlborn efficiency η_{max}^* (solid line) as a function of $\Delta T = T_1 - T_2$, where the temperature of the cold cell is kept at $T_2 = 0.5$. η_{max}^* has been scaled ($\eta_{max}^* \times 0.075$) for easy visualization of all quantities on the same plot. The inset shows the detail of the efficiency at maximum power in the linear response regime. Parameter values are $M/m = 5.0$ and $\sigma_B = 0.5$.

In terms of the load, we can write this expression as,

$$\varepsilon_{max}^* = \frac{L_{21}}{L_{11}} \frac{1}{2|F|} \quad (23)$$

However, for the BL refrigerator, $q = 1$ will never be attainable due to the kinetic energy contribution [14] and consequently ε_q^* will be less than ε_{max}^* .

These predictions of linear irreversible thermodynamics concerning η^* and ε^* have not been verified when temperature is spatially inhomogeneous. One of our objectives is to investigate the validity of linear irreversible theory via numerical simulation of the inertial Langevin equation.

From Fig. 2 we find that the power $-\dot{W}$ reaches a maximum at an optimum value of the load F^* . We then evaluate the efficiency at F^* , which is the efficiency at maximum power, as a function of ΔT .

In Fig. 11, we plot as a function of ΔT , the Curzon-Ahlborn efficiency η_{max}^* , η^* obtained from numerical solution of the inertial Langevin equation and the efficiency at maximum power predicted by linear response theory, namely η_q^* . In order to determine η_q^* we have to find q , which is evaluated from the values of the Onsager coefficients, numerically. As the kinetic energy contribution is proportional to the temperature difference, it diminishes η^* to zero as $\Delta T \rightarrow \infty$, thus contradicting the results of Ref. [7], obtained using overdamped models. There is an optimum ΔT at which η^* reaches a maximum but it is far below η_{max}^* . In the linear response regime, there is

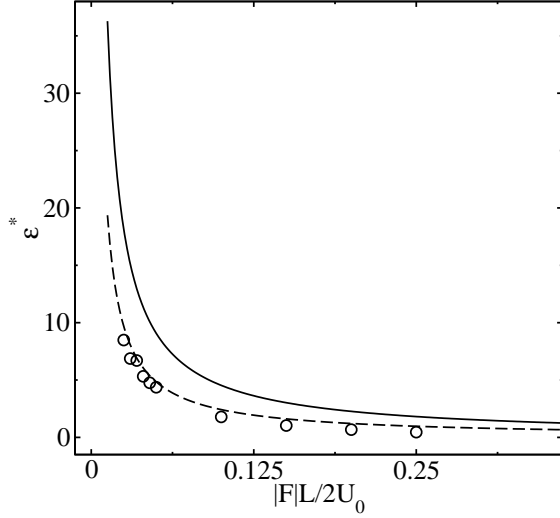


FIG. 12: ε^* obtained from numerical simulation (symbols), ε_q^* (dashed line) and ε_{max}^* (solid line), as a function of the external force. Parameter values are $M/m = 5.0$, $\sigma_B = 5.0$ and $T_1 = T_2 = 0.5$.

good agreement between η^* and η_q^* , as shown in the inset of Fig. 11b.

We now investigate the performance of the refrigerator at maximum $\dot{Q}_{2 \rightarrow 1} \Delta T / T$, numerically. The quantity $\dot{Q}_{2 \rightarrow 1} \Delta T / T$ reaches a maximum at an optimum value of the temperature difference, namely ΔT^* . Then, we evaluate the coefficient of performance ε^* at ΔT^* as a function of $|F|$. Figure 12 shows that ε^* is always lower than ε_{max}^* due to the kinetic energy contribution. There is also good agreement between ε^* and the coefficient of performance predicted by linear response theory ε_q^* .

VI. EFFICIENCY OPTIMIZATION

Figure 4 (8) showed that $\eta(\varepsilon)$ reaches a maximum at optimum values of the mass and damping between the overdamped and underdamped limits. In this regime, the efficiency can be further enhanced by reducing the kinetic energy contribution.

The major cause of the low efficiency and coefficient of performance in the BL motor and refrigerator respectively is the heat transfer due to kinetic energy across the temperature boundary. When a temperature boundary coincides with the potential minima, the situation is the worst since the Brownian particle crosses the temperature boundary many times, resulting in a large heat transfer via kinetic energy, as illustrated in Fig. 13. In order to reduce the number of crossings, we must move the temperature boundary away from the potential minima. On the other hand, the other temperature boundary should remain close to the potential maxima to maintain the current of Brownian particles.

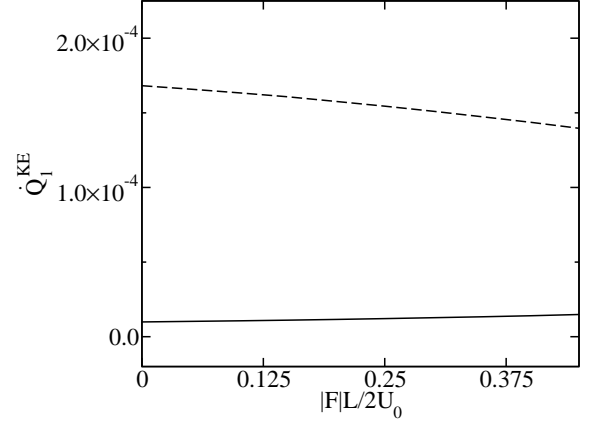


FIG. 13: Heat flow via kinetic energy at the potential minima (dashed line) and maxima (solid line) as a function of the external load. Parameter values are $T_1 = 0.7$, $T_2 = 0.3$, $M/m = 5$ and $\sigma_B = 5.0$.

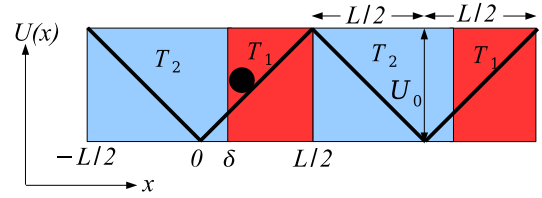


FIG. 14: (Color online) The temperature and potential profiles corresponding to *case I* of motor and refrigerator. The dark circle represents the Brownian particle.

Another way to minimize the number of crossings would be to keep the same temperature profile but modify the potential shape so that there is a small potential barrier of height $E < U_0$ at the location of the potential minima, which in our original model coincides with the temperature boundary. Since the Brownian particle is less likely to be found at a potential maxima, the number of crossings will decrease and consequently the kinetic energy contribution will become diminish.

Based on the above ideas, we will study the optimization of the BL motor and refrigerator in two different cases, where we vary the potential (*case I*) and temperature (*case II*) profiles as compared to our original model.

A. Motor

In *case I*, we shift the location of the temperature boundary away from the potential minima. The potential $U(x)$ is the same as in our original model but the temperature profile $T(x)$ is modified and is now given

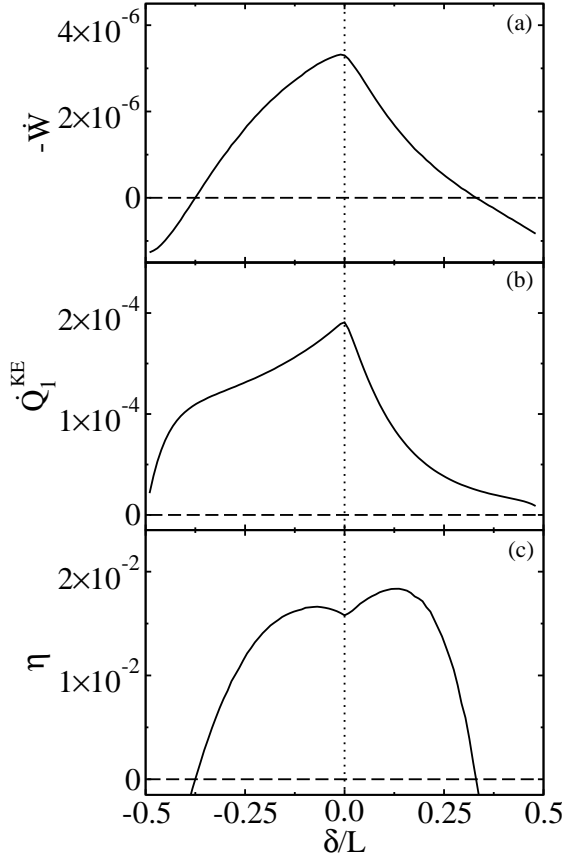


FIG. 15: (a) Power ($-\dot{W}$), (b) heat flux due to kinetic energy, and (c) efficiency of the motor as a function of δ/L for *case I* of motor obtained from the inertial Langevin equation. In (a), (b) and, (c) the thin horizontal dashed line represents $y = 0$. Parameter values are $T_1 = 0.7$, $T_2 = 0.3$, $|F|L/2U_0 = 0.1$, $M/m = 5$ and $\sigma_B = 5.0$. The Carnot efficiency $\eta_c = 0.57$.

by:

$$T(x) = \begin{cases} T_2 & \text{for } -\frac{L}{2} < x \leq \delta \\ T_1 & \text{for } \delta < x \leq L \end{cases} \quad (24)$$

where, $T_1 > T_2$ and the parameter δ specifies the location of the temperature boundary.

At $\delta/L = 0$, the cell boundary coincides with the potential maxima/minima and we go back to our previous model studied in section II. At $\delta/L = -1/2$ and $1/2$, the temperature becomes uniform since the width of the cold ($\delta/L = -1/2$)/hot ($\delta/L = 1/2$) cell goes to zero and the system ceases to work as a motor. The motor can deliver work for δ/L in the range $-1/2 < \delta/L < 1/2$. In Fig. 15, we plot the work output, heat flow and efficiency as a function of the parameter δ/L . Figure 15 clearly shows that as the cell boundary moves away from the potential minima, in either direction, the irreversible heat transfer via kinetic energy is reduced. When $\delta/L > 0$, the presence of the cold region reduces the likelihood of the Brownian particle jumping over the barrier in the positive

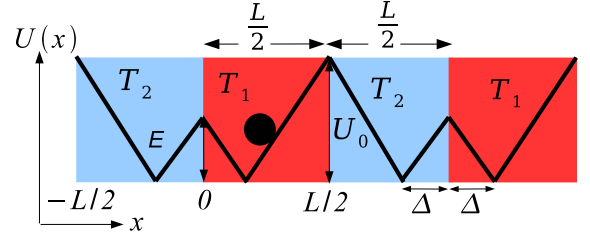


FIG. 16: (Color online) The temperature and potential profiles corresponding to *case II* of motor and refrigerator. The dark circle represents the Brownian particle.

direction, especially if $(2U_0/L)\delta \gg T_2$, thus diminishing the current and the power $-\dot{W}$, and consequently the efficiency. On the other hand if δ/L is close to the potential minima, the kinetic energy contribution becomes large, again reducing the efficiency. At an optimum $\delta/L > 0$, the efficiency is maximized as shown in Fig. 15.

When $\delta/L < 0$, the hot region extends to the left of the potential minima at $x = 0$. This enhances the probability of the Brownian particle reaching the higher-potential-energy region and crossing the barrier in the negative direction. As a result, the net particle current in the positive direction and the power delivered by the Brownian particle diminish, thus reducing the efficiency. On the other hand, if δ/L is close to $x = 0$, the large heat transfer via kinetic energy reduces the efficiency. Figure 15 shows that there is an optimum $\delta/L < 0$, at which the efficiency is maximized. However, the maximum efficiency is far below the Carnot limit.

In *case II*, we keep the same temperature profile as in our original model [Eq. (4)] but change the potential profile $U(x)$, which is now given by,

$$U(x) = \begin{cases} -\frac{2U_0}{L-2\Delta}(x + \Delta) & \text{for } -\frac{L}{2} < x \leq -\Delta \\ \frac{E}{\Delta}(x + \Delta) & \text{for } -\Delta < x \leq 0 \\ -\frac{E}{\Delta}(x - \Delta) & \text{for } 0 < x \leq \Delta \\ \frac{2U_0}{L-2\Delta}(x - \Delta) & \text{for } \Delta < x \leq \frac{L}{2} \end{cases} \quad (25)$$

Equation(25) shows that the potential has a barrier of height $E < U_0$ at $x = 0$, coinciding with the position of the potential minima in our original model.

In Fig. 17, we plot $-\dot{W}$, various components of \dot{Q}_1 and η as a function of the barrier height E at $x = 0$ normalized by U_0 . At $E/U_0 = 0$, the temperature boundary coincides with a potential minima and the kinetic energy contribution is large thus leading to a low efficiency. As we increase E/U_0 , the irreversible heat transfer via kinetic energy decreases as the recrossing of the Brownian particle near the temperature boundary at $x = 0$ is reduced on account of a potential maxima there. However, the motor velocity and consequently the power is diminished as well because the asymmetry around a potential minima due to the inhomogeneous temperature decreases. The efficiency is maximized for $0 < E/U_0 < 1$,

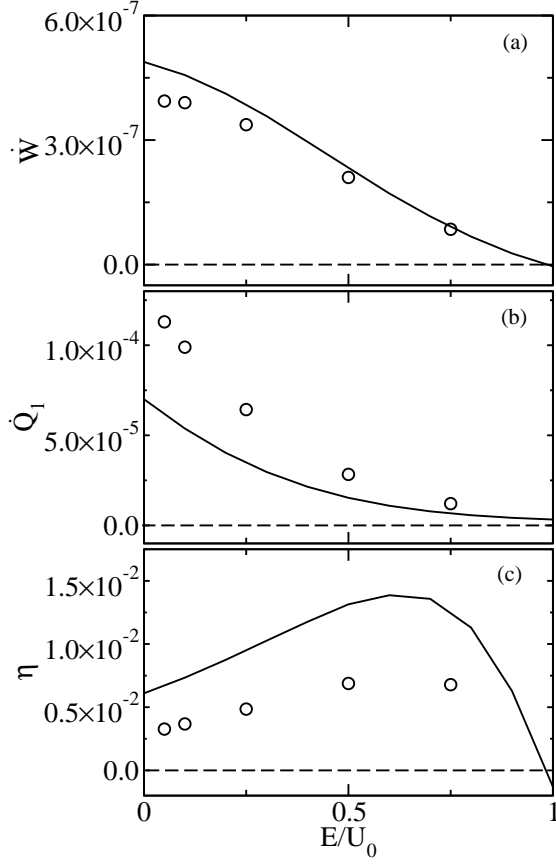


FIG. 17: (a) Power, (b) heat flux due to kinetic energy, and (c) efficiency of the motor as a function of E/U_0 for *case II* of motor. Solid lines correspond to data obtained from the inertial Langevin equation. Circles correspond to data obtained from MD simulation. In (a), (b) and, (c) the thin horizontal dashed line represents $y = 0$. Parameter values are $T_1 = 0.4$, $T_2 = 0.2$, $\Delta/L = 0.1$, $|F|L/2U_0 = 0.025$, $M/m = 5$ and $\sigma_B = 5.0$. The Carnot efficiency $\eta_c = 0.5$.

as shown in Fig. 17, though it remains far below the Carnot limit ($\eta_C = 0.5$). Figure 17 also shows qualitative agreement between the inertial Langevin equation and MD simulation.

B. Refrigerator

We now consider the performance of the BL refrigerator corresponding to the same two cases, which were introduced in the previous subsection for the BL motor.

In Fig. 18, we plot the work input, heat flow out of cell 2 and the coefficient of performance as a function of the location of the temperature boundary δ/L corresponding to *case I*. Since $\Delta T \ll 1$, the thermal gradient has a negligible effect on the particle current. Instead, the magnitude of the negative current is determined mostly by the potential shape and the external force F . How-

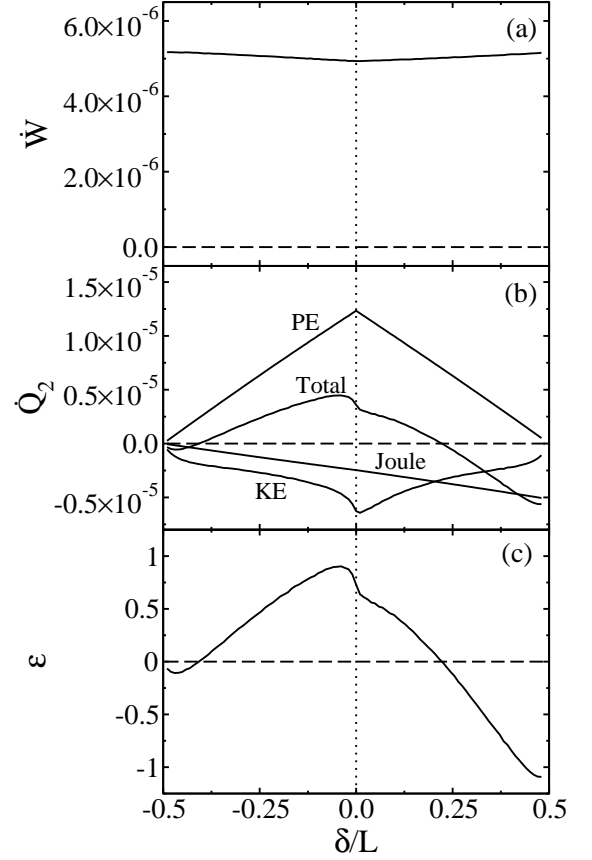


FIG. 18: (a) Work input \dot{W} , (b) various components of \dot{Q}_2 (from top to bottom, the heat flows are \dot{Q}_2^{PE} , \dot{Q}_2 , \dot{Q}_2^{J} and \dot{Q}_2^{KE}), and (c) the coefficient of performance ε of the refrigerator as a function of δ/L , corresponding to *case I* of refrigerator obtained from the inertial Langevin equation. In (a), (b) and, (c) the thin horizontal dashed line represents $y = 0$. The parameter values are $|F|L/2U_0 = 0.2$, $M/m = 5.0$ and $\sigma_B = 5.0$, $T_1 = 0.51$ and $T_2 = 0.5$. The Carnot coefficient of performance $\varepsilon_c = 50$.

ever, the potential profile stays the same regardless of the position of the temperature boundary. Hence, the power input varies slowly with δ/L , as shown in Fig. 18.

As expected, Fig. 18 shows that the kinetic energy contribution becomes smaller as the temperature boundary is shifted away from the potential minima. The joule heat dissipated to the cold cell vanishes at $\delta/L = -1/2$ since the width of the cold region goes to zero at that point. As δ/L shifts to the right of $x = -1/2$, the joule heat starts to increase as the width of the cold cell becomes larger and reaches a maximum at $\delta/L = 1/2$, when the cold cell occupies the entire period L of the potential. As the temperature boundary is shifted to the left of $\delta/L = 0$, the heat flow via potential \dot{Q}_2^{PE} , is reduced since the width of the cold cell becomes smaller and less potential energy is extracted. When $\delta/L > 0$, \dot{Q}_2^{PE} again diminishes since the cold cell now includes a portion of the negative

slope as well. Figure 19 shows that there is an optimum $\delta/L < 0$ at which the total heat extracted from cell 2 and the coefficient of performance reach a maximum, showing that this model can enhance the cooling and refrigerator performance by appropriately changing the location of the temperature boundary. However, ε is still far below the Carnot coefficient of performance.

In *case II*, the small barrier at $x = 0$ reduces the heat transfer via kinetic energy. This is clearly seen in Fig. 19, which shows the work input, heat flow out of cell 2 and ε as a function of the barrier height E at $x = 0$, normalized by U_0 . Due to the small temperature difference, the current and consequently the work input and the joule heat vary slowly with E/U_0 . On the other hand, the barrier of height E at $x = 0$ diminishes the heat flow via potential because due to the negative slope, $-E/\Delta$, an amount of heat E is dissipated each time the Brownian particle crosses the cold cell, thus reducing the magnitude of potential energy extracted to $U_0 - E$. Since, heat flow via potential decreases with E/U_0 more rapidly as compared to the kinetic energy contribution, there is no optimum value of E/U_0 and net heat extracted from cell 2 decreases monotonically from a maximum at $E/U_0 = 0$. The coefficient of performance also decreases with E/U_0 and is far below ε_c . Hence, this case does not improve the performance of the refrigerator.

VII. CONCLUSION

We studied the efficiency and coefficient of performance of the Buttiker-Landauer motor and refrigerator by numerical simulation of the inertial Langevin equation and MD simulation. Our results show qualitatively different behavior of the heat transfer, efficiency and coefficient of performance as a function of various parameters as compared to previous works based on overdamped models [7, 8] or other phenomenological approaches [9]. From extensive numerical simulations, we find that the irreversible heat flow via kinetic energy greatly reduces the motor efficiency and refrigerator coefficient of performance. As long as there is a temperature difference between the heat baths, this heat flow cannot be neglected. As a consequence, the transition point from motor to refrigerator is not at the stalled state, but when the heat transfer via potential is greater than the sum of the joule heat and the heat flow via kinetic energy. This occurs only when the load exceeds the stall load.

There is an optimal value of the mass and friction coefficient at which the efficiency/coefficient of performance reach a maximum. However, they are far below their respective Carnot limits. We also found that the efficiency at maximum power can never attain the Curzon-Ahlborn efficiency due to the irreversible heat flow via kinetic energy. Due to this irreversible heat, the coefficient of performance of the refrigerator is below the theoretical maximum predicted by linear response theory, under conditions which could be considered as the

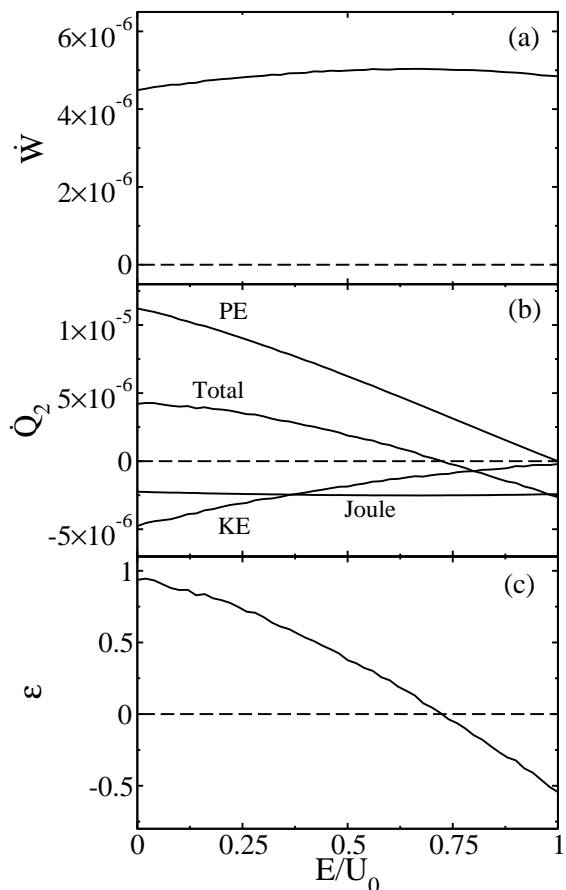


FIG. 19: (a) Work input \dot{W} , (b) various components of \dot{Q}_2 (from top to bottom, the heat flows are \dot{Q}_2^{PE} , \dot{Q}_2 , \dot{Q}_2^{J} and \dot{Q}_2^{KE}), and (c) the coefficient of performance ε of the refrigerator as a function of E/U_0 , corresponding to *case II* of refrigerator obtained from the inertial Langevin equation. In (a), (b) and, (c) the thin horizontal dashed line represents $y = 0$. The parameter values are $|F|L/2U_0 = 0.2$, $M/m = 5.0$ and $\sigma_B = 5.0$, $T_1 = 0.51$ and $T_2 = 0.5$. The Carnot coefficient of performance $\varepsilon_c = 50$.

equivalent of maximum power. The predictions of linear irreversible thermodynamics are in good agreement with numerical data. Changing potential shape or the temperature profile in order to reduce the heat flow via kinetic energy reduces the particle current as well, leading only to a small enhancement of the motor efficiency and refrigerator coefficient of performance.

Since reduction of heat transfer via kinetic energy results in diminishing the particle current thus making the motor less efficient, the next question to address is how one can reduce the irreversible heat without decreasing the particle current in order to enhance the motor efficiency and refrigerator coefficient of performance. At a more fundamental level, it would be interesting to obtain theoretically the maximum efficiency at maximum power and the equivalent maximum for the coefficient of performance. Answering such questions would also enhance

our understanding of non-equilibrium thermodynamics at the small scale.

Acknowledgments

Computer simulations were partly carried out at the Alabama Supercomputer Center. The author is pro-

foundly grateful to Prof. Ryoichi Kawai for his valuable comments and ideas for improving the manuscript and encouraging the author to write this paper. We also thank the GAFP Program of the University of Alabama at Birmingham, for financial support.

-
- [1] P. Reimann, Phys. Rep. **361**, 57 (2002).
 - [2] R. P. Feynman, R. B. Leighton, and M. Sands, *The Feynman Lectures on Physics* (Addison Wesley, Reading, MA, 1966), Vol. I, Chap. 46.
 - [3] R. Landauer, J. Stat. Phys. **53**, 233 (1988).
 - [4] M. Büttiker, Z. Phys. B **68**, 161 (1987).
 - [5] J. M. R. Parrondo and B. J. de Cisneros, Appl. Phys. A: Mater. Sci. Process. **75**, 179 (2002)
 - [6] N. G. Van Kampen, IBM J. Res. Develop, **32**, 107 (1988).
 - [7] M. Asfaw and M. Bekele, Eur. Phys. J. B **38**, 457 (2004).
 - [8] M. Asfaw and M. Bekele, Physica A **384**, 346 (2007).
 - [9] B. -Q. Ai, H. -Z. Xie, D. -H. Wen, X. -M. Liu, and L. -G. Liu, Eur. Phys. J. B **48**, 101 (2005); B. -Q. Ai, L. Wang, and L. -G. Liu, Phys. Lett. A **352**, 286 (2006).
 - [10] K. Sekimoto, J. Phys. Soc. Jpn. **66**, 1234 (1997).
 - [11] M. Matsuo and S. -I. Sasa, Physica A **276**, 188 (2000).
 - [12] I. Derényi and R. D. Astumian, Phys. Rev. E **59**, R6219 (1999).
 - [13] T. Hondou and K. Sekimoto, Phys. Rev. E **62**, 6021 (2000).
 - [14] R. Benjamin and R. Kawai, Phys. Rev. E **77**, 051132 (2008).
 - [15] C. Van den Broeck, Phys. Rev. Lett. **95**, 190602 (2005).
 - [16] F. L. Curzon and B. Ahlborn, Am. J. Phys. **43**, 22 (1975).
 - [17] B. Jimenez de Cisneros, L. A. Arias Hernandez and A. Calvo Hernandez, Phys. Rev. E **73**, 057103 (2006).
 - [18] P. Meurs, C. Van den Broeck, and A. Garcia, Phys. Rev. E **70**, 051109 (2004).
 - [19] K. Sekimoto, Prog. Theor. Phys. Suppl. **130**, 17 (1998).
 - [20] K. Sekimoto, *Stochastic Energetics* (Springer, in preparation).
 - [21] Y. M. Blanter and M. Büttiker, Phys. Rev. Lett. **81**, 4040 (1998).
 - [22] C. Van den Broeck, Adv. Chem. Phys. **135**, 189 (2007).